Letters on Materials 8 (4), 2018 pp. 435-439 www.lettersonmaterials.com

DOI: 10.22226/2410-3535-2018-4-435-439 PACS: 62.20.Fe

Gradient dislocation substructures at fracture of polycrystalline Cu-Mn alloys

N. A. Koneva†, L. I. Trishkina, T. V. Cherkasova

†koneva@tsuab.ru

Tomsk State University of Architecture and Building, 2 Solyanaya Sq., Tomsk, 634003, Russia

The paper presents the results of transmission electron microscopic (TEM) studies on the defect substructure of alloys and its modification with an increasing distance from the fracture surface. Cu-Mn polycrystalline FCC solid solutions with Mn contents of 0.4 and 25 at. % and the average grain size of 100 μm are studied. A test machine INSTRON is used to perform tensile deformation of Cu-Mn samples at room temperature and $2 \cdot 10^{-2}$ s^{-1} strain rate. The strain is measured, the types of the dislocation substructure (DSS) and their parameters are studied with the step of $2 \cdot 10^{-3}$ m in the local zones of fractured samples at different distances from the fracture surface. As a result of the experiments, the sequence of changes in the substructure with an increasing distance from the fracture surface are established. In Cu + 0.4 at. % Mn alloy the following substructural sequence is observed: micro-bands, misoriented cells, nonmisoriented cells, and dislocation tangles. Substructural change sequence in Cu + 25 at. % Mn alloy includes microbands, cell-networks with and without misorientations, dislocation pile-ups, and chaotic dislocation distributions. In both alloys terminated subboundaries have a high density near the fracture surface. It is observed that the substructures change gradually depending on the distance to the fracture surface. Substructures that cause the fracture of the alloys at a meso-scale level were also detected. Near the fracture surface, deformation boundaries are misoriented and characterized by a large amplitude of the lattice curvature-torsion. Misoriented cell and microband DSS are observed within the fracture area of Cu + 0.4 at. % Mn alloy. In Cu + 25 at. % Mn alloy the formation of misoriented cell-network DSS and microband DSS is observed. Microcracks appear both along the boundaries of misoriented substructures and grain boundaries.

Keywords: Cu-Mn alloys, tension, fracture, dislocation-disclination substructures.

1. Introduction

It is well-known that during active plastic deformation different misoriented dislocation and dislocation-disclination substructures (DDS) are formed at the strain values above $\varepsilon_{true} = 0.20 - 0.25$ [1 – 7]. These substructures are characterized by the formation of boundaries between misoriented and non-misoriented regions, terminated subboundaries, by the curvature-torsion of a crystal lattice, and internal stress fields. The dislocation-disclination substructures include such structures as microbands, one- and two-dimentional, fragmented, subgrain structures and substructures with continuous and discrete misorientations. They can have two types of misorientations, continunous and discrete ones [8].

The fracture of metallic materials is determined by the regularities of their deformation on different scales and structural levels [1,9]. It is important to establish the types of the substructure, the changes in their quantitative characteristics with a distance from the fracture zone, which would make it possible to estimate the strength and ductility of materials of a given class at high loads. Such studies were partially carried out for steels. No detailed studies describing the quantitative characteristics of substructures at considerable distances from the fracture zones has been performed for Cu-Mn alloys.

The present work is aimed at electron microscopic studies of the change in the defect structure and its parameters with a distance from the fracture zones and establishing the types of DDS determining the fracture of metallic materials on the mesoscopic level.

2. Materials and experimental procedures

Polycrystalline FCC solid solutions Cu-Mn with Mn content of 0.4 and 25 at. % with the average grain size of 100 μm were taken as materials for the study. The samples of alloys were deformed in tension at room temperature at the strain rate of $2 \cdot 10^{-2}$ s^{-1} using an "Instron" test machine. The defect structure was studied by means of transmission electron microscopy (TEM) on a microscope with the accelerating voltage of 125 kV having a goniometer at the magnification of 25000. The study of the defect structure and its parameters was carried out in local zones of the samples at varying distances from the fracture surface with a step of $2 \cdot 10^{-3}$ m. The strain level ε^{1}_{true} was determined for every local zone of the samples. The intercept method [10] was used to measure the dislocation density, density of subboundaries, microbands, and microcracks. Curvature of the crystal lattice (χ) is an important parameter of the defect structure [5,9,11,12]. In the general case, χ is a second-rank tensor [13,14], which contains the components of curvature

and torsion of the crystal lattice. Therefore, it is reasonable to define χ as the curvature-torsion. Experimentally, the values of χ are determined from the gradient of a continuous misorientation in a crystal. Here, it was measured by the electron-microscopic method using bend extinction contours [11,15] as follows:

$$\chi = \frac{\partial \varphi}{\partial \ell},$$

where φ is the tilt angle of a crystallographic plane with respect to the electron beam, ℓ is the distance in the crystal. The details of measurements of $\Delta\varphi/\Delta\ell$ are given elsewhere [14,15]. It should be noted that to measure χ and the related density of geometrically necessary dislocations electron backscattered diffraction (EBSD) method is used nowadays [16,17].

3. Results and discussion

Fig. 1 schematically shows the samples in their initial state and after deformation. The alloy with a Mn content of 0.4 at. % failed at the strain $\varepsilon_{true} = 0.60$, while the concentrated alloy (25 at. % of Mn) at $\varepsilon_{true} = 0.80$. In the fracture zone of the sample of Cu + 0.4 at. % Mn alloy a misoriented cell DDS and microband DDS are observed. The misoriented cell DDS is characterized by an existence of misorientations between neighboring cells. Such a substructure is observed at the distances of up to $4 \cdot 10^{-3}$ m from the fracture surface of the sample, which corresponds to the local strain of $\varepsilon^{1}_{true} = 0.15$. Misorientations between the groups of dislocation cells are observed at the distances of up to $6 \cdot 10^{-3}$ m from the fracture surface, which corresponds to the local deformation $\varepsilon^{1}_{true} = 0.50$ (Fig. 2a). A microband DDS can form along misoriented cell boundaries. The microbands are observed in the fracture zone near grain boundaries (Fig. 2b). Studies show that with an increasing distance from the fracture zone of Cu + 0.4 at. % Mn alloy the formation of dislocation structures in the following sequence is observed: a microband DDS, a misoriented cellular DDS, a nonmisoriented cellular DDS, dislocation tangles. Microcracks formed along the misoriented cell boundaries, microbands, and grain boundaries are observed near the fracture zone.

Fig. 2 also shows the types of DDS that are observed in the fracture zone of Cu + 25 at. % Mn alloy: a misoriented cell-network DDS (Fig. 2c) and a microband DDS (Fig. 2d). The following types of substructures are formed with an increasing distance from the fracture zone: microband, misoriented cell-network, nonmisoriented cell-network, network, dislocation tangles, and random distributions of dislocations. Microcracks formed along the microbands and grain boundaries are observed in the fracture zone (Fig. 2f). It should also be noted that near the fracture zone terminated subboundaries that are descried as partial disclinations are observed [1,18].

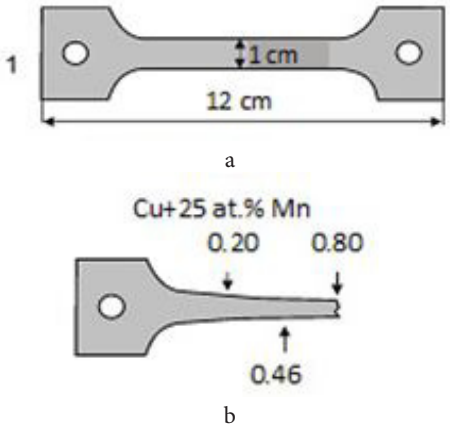

Fig. 1. Schematics of the specimens of alloys: original state (a); after deformation (b).

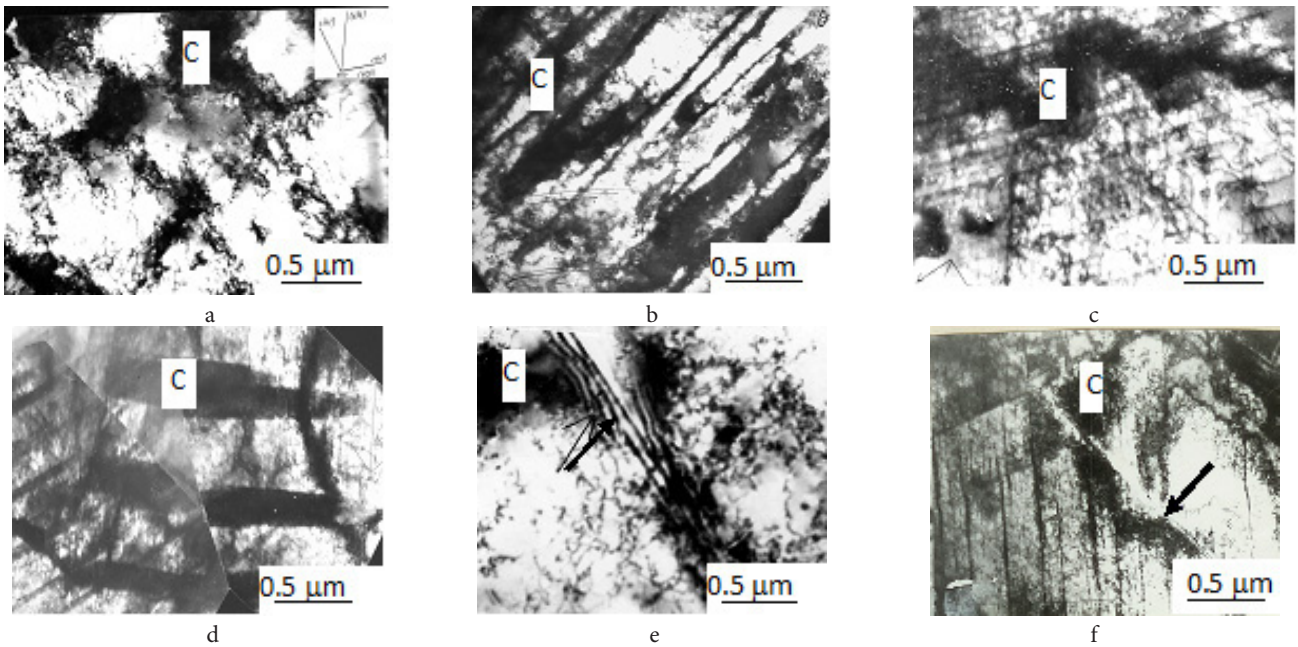

Fig. 2. TEM images of dislocation substructures in fracture zones in Cu + 0.4 at. % Mn (a, b, e) and Cu + 25 at. % Mn (c, d, f) alloys: misoriented cells (a), micro-bands (b), misoriented cell-networks (c), microbands (d), microcracks along cell boundaries (e), microcracks along grain boundaries (f); C — extinction contours due to strains.

The change in parameters characterizing the DDS was also performed in local zones of the samples at every $2 \cdot 10^{-3}$ m from the fracture surface. The density of dislocations ρ in various components of the defect substructure (in nonmisoriented and misoriented cell structures, cell-network and microband structures), the curvature-torsion of the crystal lattice χ, density of terminated subboundaries and microcracks were measured.

Presented in Fig. 3 are the dependencies of the scalar density of dislocations in different substructures on the distance X from the fracture surface for both alloys. The strain interval corresponding to the studied interval of distances amounted $\varepsilon^1_{true} = 0.60 - 0.15$ for Cu + 0.4 at.% Mn alloy and $\varepsilon^1_{true} = 0.80 - 0.15$ for Cu + 25 at.% Mn alloy. The analysis of the dependences shows that in Cu + 0.4 at.% Mn alloy up to the distance of $6 \cdot 10^{-3}$ m from the fracture surface a sharp decrease of the density of dislocations in all DDS is observed and with a further increase of the distance this decrease slows down (Fig. 3a). A similar behavior of dependences $\rho = f(X)$ is observed for the Cu + 25 at.% Mn alloy (Fig. 3b).

A common feature for the alloys under consideration is that the density of dislocations in the microband DDS is higher than that in misoriented cellular and misoriented cell-network structures.

Fig. 4 presents the changes in the density of the microbands, terminated subboundaries and microcracks with the distance from the fracture surface for the Cu + 0.4 at.% Mn alloy. As one can see from the figure, the density of terminated subboundaries is twice higher than that of the microbands. The abovementioned parameters have the largest values immediately near the fracture surface and up to the distance of $4 \cdot 10^{-3}$ m from it and then with the further increase of the distance the parameters decrease slowly with a subsequent saturation. Such dependencies are characteristic of the Cu + 25 at.% Mn alloy as well (Fig. 5).

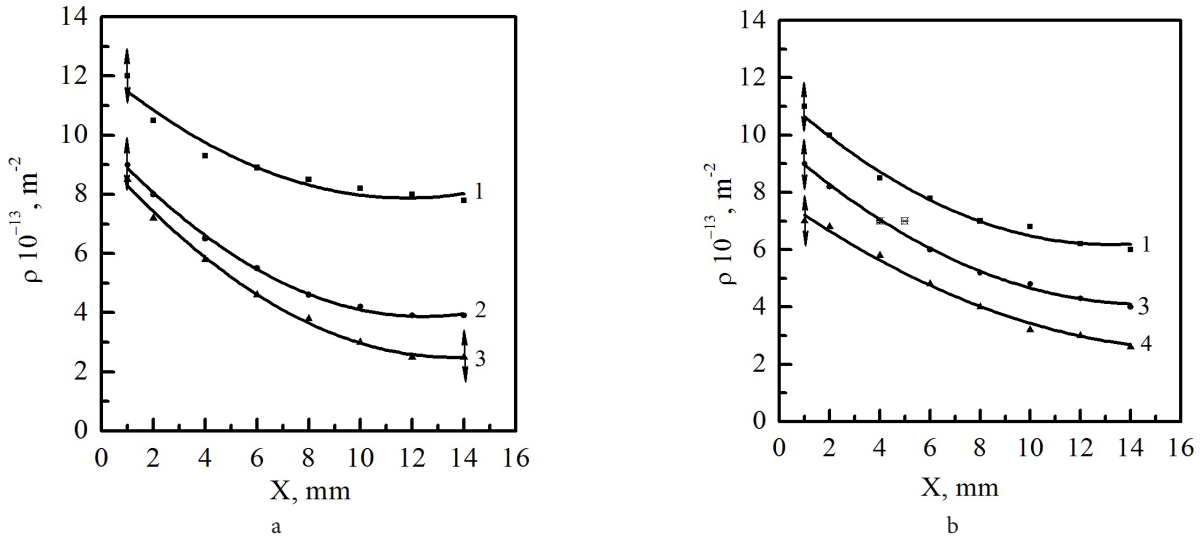

Fig. 3. Dependences of the dislocation density ρ in different substructures on the distance from fracture surfaces X in Cu + 0.4 at.% Mn (a) and Cu + 25 at.% Mn (b) alloys: 1 — microbands; 2 — misoriented cells; 3 — misoriented cell-networks; 4 — terminated boundaries.

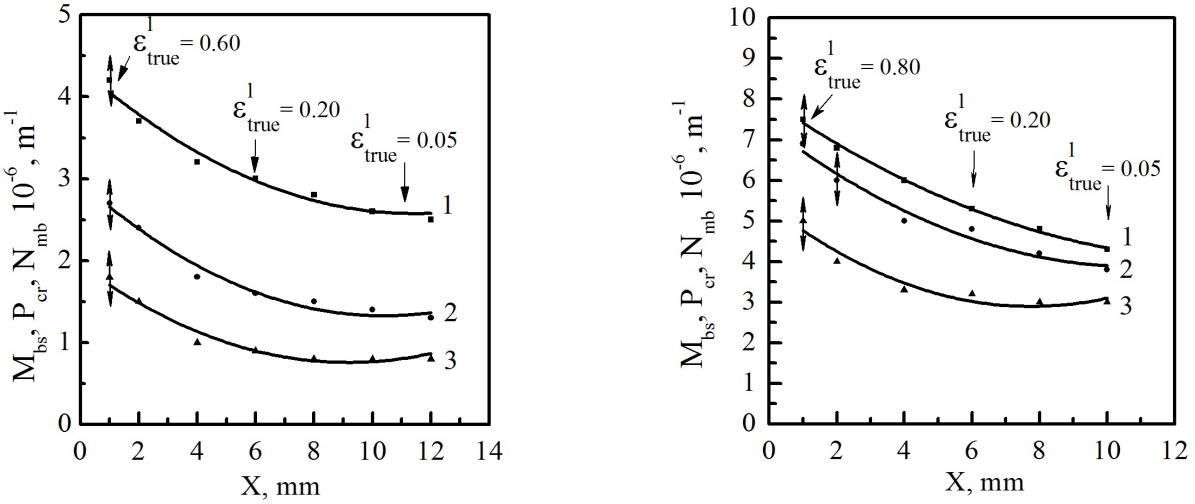

Fig. 4. Dependences of parameters characterizing DSS in Cu + 0.4 at.% Mn alloy on the distance from a fracture zone X: 1 — density of terminated subboundaries M_{bs}; 2 — density of microbands N_{mb}, 3 — density of microcracks P_{cr}.

Fig. 5. Dependences of DSS parameters in Cu + 25 at.% Mn alloy on the distance from a fracture surface X: 1 — density of terminated sub-boundaries M_{bs}; 2 — density of microbands N_{mb}, 3 — density of microcracks P_{cr}.

Measurements of the crystal lattice curvature-torsion were also carried out in the local zones at increasing distances from the fracture surface of the samples. Fig. 6 demonstrates the changes of the values of χ with the distance measured experimentally for different sources of the crystal distortion. One can see that χ decreases with the distance X and has the highest values near the fracture zone in both alloys. It also should be noted that the value of χ from terminated subboundaries, microbands and microcracks is higher in the Cu + 25 at. % Mn alloy. Fairly high values χ are characteristic of terminated subboundaries and microband DDS. Up to the $4 \cdot 10^{-3}$ m distance from the fracture zone the decrease of χ is more intensive, and then the dependencies $\chi = f(X)$ reach a saturation. The density of the microcracks has larger values up to the distance $4 \cdot 10^{-3}$ m from the fracture surface, and then the density falls smoothly. At the distance of more than $6 \cdot 10^{-3}$ microcracks are no more observed.

The analysis of the results obtained shows that by the moment of the fracture of alloys a considerable inhomogeneity of the plastic deformation is developed. This inhomogeneity correlates with the formation of the gradient of misoriented DDS. In the zone of fracture microcracks along the microbands, misoriented cell boundaries and grain boundaries are observed. With that, in the Cu + 25 at. % Mn alloy the values of ε^{l}_{true} in the fracture zone is significantly higher than in the Cu + 0.4 at. % Mn alloy (Fig. 1). One can assume that the reason for this is related to the fact that in a low-alloyed material a misoriented cell DDS is developed more rapidly with the strain [19] and microcracks are formed along the cell boundaries of this structure. Due to a significant solid solution hardening in a high-concentrated alloy [20,21], the dislocation structure in such an alloy is fairly homogeneous up to higher strains and the cell DDS does not form. Microcracks form along the boundaries of microbands that are formed at larger strains than in the Cu + 0.4 at. % Mn alloy. The feature common for both alloys under consideration is the formation of microcracks along the grain boundaries.

4. Conclusion

The types of DDSs forming in local zones of samples of Cu + 0.4 at. % Mn and Cu + 25 at. % Mn alloys have been determined by TEM at different distances from the fracture zone with a step of $2 \cdot 10^{-3}$ m. The parameters of DDS characterizing each type of the substructures observed have been measured. A gradient character of changes in DDSs with the distance from the fracture zone has been revealed. It has been established that in the alloys studied deformation induced misoriented boundaries are observed near the fracture surface. In Cu + 0.4 at. % Mn alloy these are boundaries of misoriented cells, microbands, terminated subboundaries and in Cu + 25 at. % Mn alloy microbands and terminated subboundaries. The highest values of crystal lattice curvature-torsion are observed near the terminated subboundaries. Values of the curvature-torsion induced by terminated subboundaries, microbands and microcracks are higher in the Cu + 25 at. % Mn alloy than those in the Cu + 0.4 at. % Mn alloy. The main sources of microcracks observed on the mezoscale level are misoriented cell and microband boundaries in the Cu + 0.4 at. % Mn alloy, and microband boundaries Cu + 25 at. % Mn. Grain boundaries are common sources of the microcrack formation in both alloys.

Acknowledgements. The present work was accomplished in the frame of a state assignment research project #3.8320.2017/BCh.

References

1. V. V. Rybin. Large Plastic Deformations and Fracture of Metals. Metallurgia, Moscow (1986). 224 p. (in Russian)
2. V.I. Trefilov, V.F. Moiseev, E.P. Pechkovski et al. Deformation Hardening and Fracture of Polycrystalline Materials. Naukova Dumka, Kiev (1989) 256 p. (in Russian)

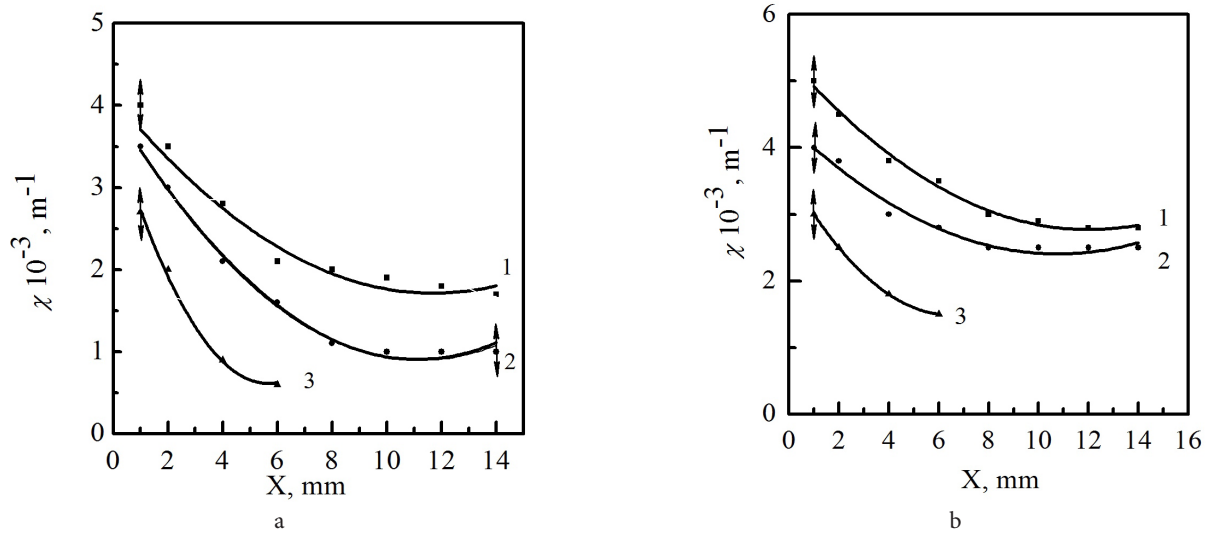

Fig. 6. Dependences of the lattice curvature-torsion χ induced by different sources on the distance from a fracture zone X in Cu + 0.4 at. % Mn (a); Cu + 25 at. % Mn (b) alloys: 1 — near terminated boundaries; 2 — micro-bands; 3 — microcracks.

3. N. A. Koneva, D. V. Lychagin, L. A. Teplyakova, E. V. Kozlov. In: Theoretical and Experimental Study of Disclinations (Ed. V. I. Vladimirov). A. F. Ioffe Physico-Technical Institute, Leningrad (1986) P. 116 – 126. (in Russian)
4. N. A. Koneva, E. V. Kozlov. Structural Levels of Plastic Deformation and Fracture (Ed. V. E. Panin). Nauka, Novosibirsk (1990) P. 123 – 186. (in Russian)
5. E. V. Kozlov, N. A. Koneva, L. I. Trishkina. In: Disclinations and Rotation Deformation of Solids (Eds. A. E. Romanov). A. F. Ioffe Physico-Technical Institute, Leningrad (1990) P. 89 – 125. (in Russian)
6. D. Kuhlmann-Wilsdorf. Phil. Mag. A. 79(4), 955 (1999).
7. E. Nes. Progr. Mater. Sci. 41, 129 (1998).
8. N. A. Koneva, E. V. Kozlov, L. I. Trishkina. Metallofizika. 13(10), 49 (1991). (in Russian)
9. V. E. Panin, A. V. Panin, T. Ph. Elsukova, Yu. Ph. Popkova. Physical Mesomechanics. 18(2), 89 (2015).
10. S. A. Saltykov. Stereometric Metallography. Metallurgia, Moscow (1970) 376 p. (in Russian)
11. N. A. Koneva, S. F. Kiseleva, N. A. Popova, E. V. Kozlov. Fundamental'nye Problemy Sovremennogo Materialovedeniya 3, 34 (2011). (in Russian)
12. A. N. Tumentsev, I. A. Ditenberg, A. D. Korotaev, K. I. Denisov. Physical Mesomechanics. 16(4), 319 (2013).
13. M. A. Shtremel. Strength of Alloys. Lattice Defects. Metallurgia, Moscow (1982) 280 p. (in Russian)
14. N. A. Koneva, S. F. Kiseleva, N. A. Popova. Structural Evolution and Internal Stress Fields. Lambert Academic Publishing, Saarbrucken (2017) 148 p.
15. N. A. Koneva, L. I. Trishkina, D. V. Lychagin, E. V. Kozlov. New Methods in Physics and Mechanics of Deforming Solids. Part I. (Ed. V. E. Panin). Tomsk State University, Tomsk (1990) P. 83 – 93. (in Russian)
16. M. Calcaynotto, D. Ponge, E. Demir, D. Raabe. Mater. Sci. Eng. A. 527, 2738 (2010).
17. A. Kundu, D. P. Field. Mater. Sci. Eng. A. 667, 435 (2016).
18. V. N. Perevezentsev, V. V. Rybin. Structure and Properties of Grain Boundaries. Niznii Novgorod University, Niznii Novgorod (2012) 307 p. (in Russian)
19. N. A. Koneva, E. V. Kozlov, L. I. Trishkina, T. V. Cherkasova. Fundamental'nye Problemy Sovremennogo Materialovedeniya 13(2), 162 (2016). (in Russian)
20. E. V. Kozlov, N. A. Koneva, L. I. Trishkina. Crystallografia 54(6), 981 (2009). (in Russian)
21. N. A. Koneva, L. I. Trishkina, T. V. Cherkasova. Letters on Materials 7(3), 282 – 286 (2017). (in Russian)